

**STUDYING A MODEL FOR ENERGY HARVESTING FROM MECHANICAL VIBRATIONS****NGHIÊN CỨU MÔ HÌNH KHAI THÁC NĂNG LƯỢNG TỪ RUNG ĐỘNG CƠ HỌC****Van Hai Nguyen**

Institute of Mechanics, Vietnam Academy of Science and Technology, Hanoi, Vietnam

Ngày nhận bài: 02/04/2025, Ngày chấp nhận đăng: 20/04/2025, Phản biện: GS.TSKH. Nguyễn Tiến Khiêm

**Tóm tắt:**

The paper presents the initial results achieved in the study, calculation, and establishment of an energy harvesting model from mechanical vibrations. The calculations show the stable and unstable operating regions, as well as the vibration range of the model. The power level of the model received from the mechanical vibration of the environment is determined. The device model is fabricated, and its operation is tested under the influence of mechanical vibration caused by the rotating rotor. The voltage level generated by the device is measured and evaluated.

**Từ khóa:**

Renewable energy, vibrating energy, power conversion, and electrical generator from vibration.

**Abstract:**

Bài báo trình bày các kết quả bước đầu đạt được trong nghiên cứu, tính toán và thiết lập mô hình khai thác năng lượng từ rung động cơ học. Các tính toán chỉ ra vùng hoạt động ổn định và không ổn định, phạm vi rung động của mô hình. Xác định mức công suất của mô hình thu được từ rung động cơ học của môi trường. Chế tạo mô hình thiết bị và thử nghiệm sự hoạt động của thiết bị dưới tác động của rung động cơ học do rotor chuyển động quay gây ra. Đo và đánh giá mức điện áp do thiết bị phát ra.

**Keywords:**

Năng lượng tái tạo, năng lượng rung động, chuyển đổi năng lượng và máy phát điện từ rung động.

**1. INTRODUCTION**

Nowadays, the harvesting of mechanical vibration energy from the environment has been initially studied and applied in practice. On the other hand, in daily life, all devices require electricity to operate. Therefore, the exploitation of energy from vibrating sources in the environment is necessary. In fact, these vibrating sources always exist around us, such as vibrations

in towers, traffic structures, or operating machinery. These vibration sources are primarily harmful. To overcome this disadvantage, vibrating energy can be exploited and converted into electricity. Exploiting vibration energy to generate electricity not only provides power for use but also reduces vibration-induced damage, contributing to the prolonged life-span of machinery and construction

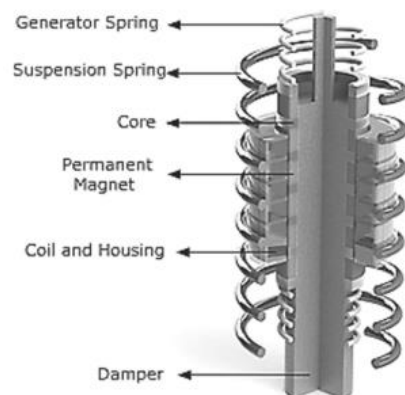
structures during operation.

Globally, the study and exploration of energy harvesting models from vibrations to generate electricity have garnered interest and are beginning to be applied in practice. In [1,2], the authors propose models for harvesting energy from vibrations generated by humans and moving vehicles. The authors use piezoelectric materials and electric motors to generate electricity under the influence of vibration forces. In [3], the authors calculated and developed a model using piezoelectric materials to determine the power and voltage levels obtained from mechanical vibration energy. In [4], the authors proposed a nonlinear vibration model using multilayer piezoelectric materials, examining the received electrical energy level according to the damping coefficient and the received voltage level according to the oscillation range of the model. In [5], the authors propose a mechanical model for a vibrational energy harvester. The authors calculate the stable operating range of the model, the correlation between force amplitude and the frequency of the applied external force, and the received voltage level according to amplitude and frequency of the model. In [6], the model for exploiting vibration energy installed on vehicles is proposed. The authors calculate the efficiency of using the the linear generator and exploit vibrations in the resonance region of the model to obtain the most optimal energy. In [7], the authors present an overview of the energy harvesting system utilizing air environment vibrations based on the piezoelectric effect. In [8], the authors study and test electromagnetic shunt

dampers for vibration suppression and energy harvesting from mechanical vibrating structures. In [9], the authors propose a model structure to harness vibration energy from the environment, establish the motion equation, and determine the optimal control of the model parameters to maximize the received energy. In [10], the authors review studies on electromagnetic vibrational energy harvesters and demonstrate their full potential. Fig. 1 illustrates various representative models of vibration-based energy harvesting that are currently being studied, fabricated, and tested worldwide.



a. The model uses piezoelectric materials [1]



b. The model uses a linear generator [6]

**Figure 1. Some models for harvesting energy from environmental vibrations**

In this paper, the author calculates and analyzes a model for harvesting energy from mechanical vibrations. The model is developed using a linear generator, which is installed to capture vibration energy produced by the rotating rotor. The generator part is set up with a stationary coil, while the magnet shaft moves back and forth in the stationary coil to generate electricity.

Through calculations, the author establishes the equations of motion, examines the stable operation of the model, and determines the range of oscillation as well as the power level of the device model based on mechanical vibrations. After that, the device is fabricated and tested for operational efficiency, with measurements taken to evaluate the voltage level generated.

## 2. ESTABLISHING THE EQUATIONS OF MOTION AND CALCULATING THE STABILITY OF THE MODEL

The mechanical vibration energy harvesting model is designed to utilize the permanent magnet shaft that moves back and forth inside the stationary coil to generate electricity. The structure of the model is shown in Fig. 2, where the vibration force  $F_0 \cos \Omega t$  is caused by the rotating rotor due to imbalance. This force is transmitted from the machine base to the beam, causing both the beam and the magnet to oscillate.

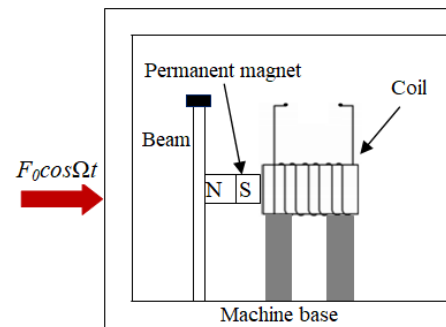


**Figure 2. Energy-harvesting model using a linear generator**

Based on the structure of the model (see Fig. 2), the mechanical model of the device is shown in Fig. 3.

The mechanical model of the energy-harvesting system consists of the magnet shaft fixed on the beam, which is simplified as an object of mass  $m$  vibrating under the influence of the vibration force transmitted from the machine base.

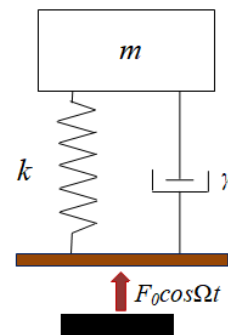


**Figure 3. Mechanical model of the device**

The governing equation of the model, as illustrated in Fig. 3, can be written as follows:

$$m \frac{d^2x}{dt^2} + \gamma \frac{dx}{dt} + k_1 x + k_2 x^3 = F_0 \cos \Omega t, \quad (1)$$

where  $m$  is the total mass of the beam and the permanent magnet shaft;  $\gamma$  is the damping coefficient;  $k_1$  is the linear stiffness coefficient;  $k_2$  is the nonlinear stiffness coefficient, influenced by the interaction between the current and the magnetic field. This interaction results in a magnetic force acting on the magnet shaft during its movement; and  $F_0$  is the amplitude, and  $\Omega$  is the frequency of the external force.

We set the variables

$$\mu^2 = \frac{k_1}{m}; h = \frac{\gamma}{m}; \beta = \frac{k_2}{m}; \text{ and } F = \frac{F_0}{m}, \quad \text{then}$$

substitute them into Eq. (1) to obtain:

$$\frac{d^2x}{dt^2} + \mu^2 x = F \cos \Omega t - h \frac{dx}{dt} - \beta x^3. \quad (2)$$

Consider the near-resonance case, with  $\Omega^2 = \mu^2 + \sigma$ . By transforming Eq. (2), we obtain:

$$\frac{d^2x}{dt^2} + \Omega^2 x = f(x, \dot{x}, \Omega t), \quad (3)$$

where the function  $f(x, \dot{x}, \Omega t)$  is given by the following expression:

$$f(x, \dot{x}, \Omega t) = -h \frac{dx}{dt} + \sigma x - \beta x^3 + F \cos \Omega t.$$

Transform Eq. (3) into the Lagrange-Bogolyubov standard form using transformation [11]:

$$x = a \cos(\Omega t + \alpha). \quad (4)$$

By calculating the derivative of Eq. (4), we obtain:

With the constraint equation [11]:

$$\frac{da}{dt} \cos(\Omega t + \alpha) - a \frac{d\alpha}{dt} \sin(\Omega t + \alpha) = 0 \quad (5)$$

Therefore, we obtain the following result:

$$\frac{dx}{dt} = -a\Omega \sin(\Omega t + \alpha) \quad (6)$$

Taking the derivative of Eq. (6) with respect to  $t$ , we obtain:

$$\frac{d^2x}{dt^2} = -\frac{da}{dt} \Omega \sin(\Omega t + \alpha) - a\Omega^2 \cos(\Omega t + \alpha) - a\Omega \frac{d\alpha}{dt} \cos(\Omega t + \alpha) \quad (7)$$

Substituting Eqs. (4), (6), and (7) into Eq. (3), we obtain:

$$-a\Omega \sin(\Omega t + \alpha) - a\Omega \frac{d\alpha}{dt} \cos(\Omega t + \alpha) = f(x, \dot{x}, \Omega t) \quad (8)$$

From Eqs. (5) and (8), we obtain the system of equations that determines  $\frac{da}{dt}$

and  $a \frac{d\alpha}{dt}$  as follows:

$$\begin{aligned} \frac{da}{dt} \cos(\Omega t + \alpha) - a \frac{d\alpha}{dt} \sin(\Omega t + \alpha) &= 0, \\ -a\Omega \sin(\Omega t + \alpha) - a\Omega \frac{d\alpha}{dt} \cos(\Omega t + \alpha) &= f \begin{pmatrix} a\Omega \cos(\Omega t + \alpha), \\ -a\Omega \sin(\Omega t + \alpha), \Omega t \end{pmatrix}. \end{aligned} \quad (9)$$

Performing the calculation, we obtain the system of equations that defines  $\frac{da}{dt}$  and

$a \frac{d\alpha}{dt}$  as follows:

$$\begin{aligned} \frac{da}{dt} &= -\frac{1}{\Omega} f(a \cos(\Omega t + \alpha), -a\Omega \sin(\Omega t + \alpha), \Omega t) \sin(\Omega t + \alpha), \\ a \frac{d\alpha}{dt} &= -\frac{1}{\Omega} f(a \cos(\Omega t + \alpha), -a\Omega \sin(\Omega t + \alpha), \Omega t) \cos(\Omega t + \alpha). \end{aligned} \quad (10)$$

To determine the solution of Eq. (10), we perform a change of variables by setting  $\Psi = \Omega t + \alpha$ , thereby obtaining  $\Omega t = \Psi - \alpha$ . By carrying out the calculation, we arrive at the following result:

$$\begin{aligned}\frac{da}{dt} &= -\frac{1}{\Omega} \left( \begin{array}{l} ha\Omega \sin \Psi + \sigma a \cos \Psi \\ -\beta a^3 \cos^3 \Psi + F \cos \Psi \cos \alpha \\ + F \sin \Psi \sin \alpha \end{array} \right) \sin \Psi, \\ a \frac{d\alpha}{dt} &= -\frac{1}{\Omega} \left( \begin{array}{l} ha\Omega \sin \Psi + \sigma a \cos \Psi \\ -\beta a^3 \cos^3 \Psi + F \cos \Psi \cos \alpha \\ + F \sin \Psi \sin \alpha \end{array} \right) \cos \Psi.\end{aligned}\quad (11)$$

We denote the expression as follows:

$$\begin{aligned}G(a, \alpha, \Psi - \alpha) &= ha\Omega \sin \Psi + \sigma a \cos \Psi \\ &\quad - \beta a^3 \cos^3 \Psi + F \cos \Psi \cos \alpha \\ &\quad + F \sin \Psi \sin \alpha.\end{aligned}$$

Applying the averaging method in nonlinear mechanics, Eq. (11) is expressed in the following form:

$$\begin{aligned}\frac{da}{dt} &= -\frac{1}{\Omega} \frac{1}{2\pi} \int_0^{2\pi} G(a, \alpha, \Psi - \alpha) \sin \Psi d\Psi, \\ a \frac{d\alpha}{dt} &= -\frac{1}{\Omega} \frac{1}{2\pi} \int_0^{2\pi} G(a, \alpha, \Psi - \alpha) \cos \Psi d\Psi.\end{aligned}\quad (12)$$

By performing the calculation on Eq. (12), we obtain:

$$\begin{aligned}\frac{da}{dt} &= -\frac{1}{2\Omega} (ha\Omega + F \sin \alpha), \\ a \frac{d\alpha}{dt} &= -\frac{1}{2\Omega} \left( \sigma a - \frac{3}{4} \beta a^3 + F \cos \alpha \right).\end{aligned}\quad (13)$$

In the case where  $\frac{da}{dt} = 0$  and  $\frac{d\alpha}{dt} = 0$ , we obtain the expressions to determine the stationary solution:

$$F \sin \alpha_0 = -ha_0 \Omega,$$

$$F \cos \alpha_0 = a_0 \left( \frac{3}{4} \beta a_0^2 - \sigma \right). \quad (14)$$

By solving Eq. (14), we obtain the equation that defines the relationship between amplitude and frequency of the model in the following form:

$$\Omega^2 = \frac{3}{4} \beta a_0^2 + \mu^2 \pm \sqrt{\frac{F^2}{a_0^2} - h^2 \Omega^2} \quad (15)$$

Fig. 4 shows graphs representing the dependence between amplitude  $a_0$  and frequency  $\Omega^2$ , with the parameters set as follows:  $m = 0.3$  kg;  $F_0 = 34$  N;  $k_1 = 110$  N/m, and  $k_2 = 190$  N/m<sup>3</sup>, in cases where the damping coefficient  $\gamma$  varies.

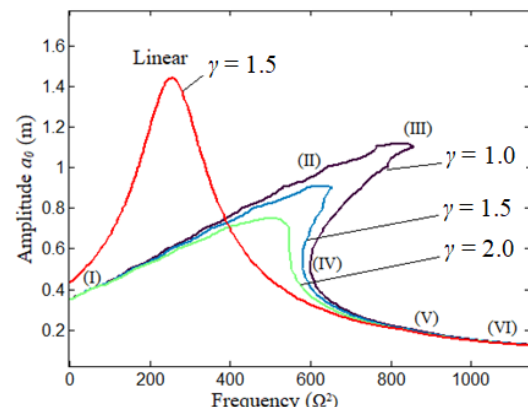


Figure 4. The resonance curve graph depicts amplitude versus frequency  $\Omega^2$

From Eq. (15) and the graphs in Fig. 4, it can be observed that for each damping coefficient  $\gamma$ , the amplitude curve of the system varies as a function of frequency  $\Omega^2$  and exhibits complexity. Specifically, in the case of the amplitude-frequency curve with a damping coefficient  $\gamma = 1.0$ , the graph shows that as  $\Omega^2$  increases, the stationary oscillation amplitude  $a_0$  takes

values along the branch extending from point (I) through point (II) to point (III). At point (III), instability occurs, causing the oscillation amplitude to drop to point (V), and then take values along the branch extending from point (V) to point (VI). As  $\Omega^2$  decreases, the stationary oscillation amplitude takes values along the decreasing branch extending from point (VI) through point (V) to point (IV).

At point (IV), there is a phenomenon where the oscillation amplitude jumps from point (IV) to point (II), then takes values along the branch extending from point (II) to point (I). At point (IV), there is a phenomenon where the oscillation amplitude jumps from point (IV) to point (II), then takes values along the branch extending from point (II) to point (I).

Therefore, in general, the stable oscillation region corresponds to the branch where the oscillation amplitude lies within the frequency range from point (I) to point (II) and from point (V) to point (VI). In the frequency region increasing from point (II) to point (III) and decreasing from point (V) to point (IV), the oscillation of the system undergoes a level jump, resulting in an unstable oscillation amplitude. This is the critical region that should be avoided when designing an operational device.

On the other hand, if sufficient data on environmental vibration is available, a model can be fabricated to operate within the stable frequency region near point (II), maximizing the oscillation amplitude and

the energy harvested from environmental vibrations. Therefore, the energy harvesting device model should be designed to function in the stable frequency region near point (II), ensuring that the system receives the maximum and most consistent amount of energy.

In addition, in practice, to ensure the long-term operation of the device model in ever-changing environmental conditions, the device should be designed to function effectively within the frequency range from point (I) to point (II) or from point (V) to point (VI). Therefore, the device will operate stably, safely, and efficiently.

### 3. INVESTIGATING THE OPERATION OF THE MODEL

When calculating the mechanical power level  $P$ , the power of the model obtained from mechanical vibration is determined by the expression [12,13]:

$$P = \frac{1}{\tau} \int_0^\tau \gamma \dot{x}(t)^2 dt, \quad (16)$$

where  $\tau$  is the time interval.

Eq. (1) can be solved numerically to obtain the response  $x = x(t)$  and  $\dot{x} = \dot{x}(t)$ . Using the Runge-Kutta algorithm implemented in the Matlab programming language, we obtain the time evolution of the response, as presented in Fig. 5 and Fig. 6.

In the calculation, the parameters are defined as follows:  $m = 0.3$  kg;  $\gamma = 2$

$\text{Ns/m}$ ;  $F_0 = 34 \text{ N}$ ;  $k_1 = 110 \text{ N/m}$ ;  $k_2 = 190 \text{ N/m}^3$ ; and the frequency  $f = 10 \text{ Hz}$  is chosen based on the stability calculation results of the model and the steel material used to fabricate the beam.

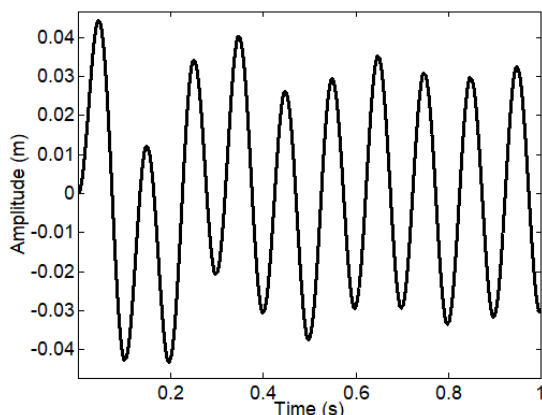


**Figure 5. The oscillation of the model versus time**

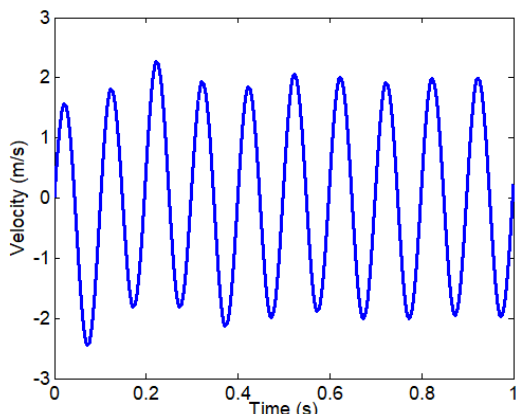


**Figure 6. The oscillatory velocity of the model versus time**

From the obtained graph results (see Fig. 5 and Fig. 6), we can determine the oscillation range of the system and the oscillatory velocity of the magnet shaft when designing the experimental model.

To determine the mechanical power level  $P$  of the model, Eqs. (1) and (16) are solved numerically using the Runge-Kutta

and Simpson methods, with the external force of the rotating rotor, which is set at a frequency of 10 Hz, acting on the model. Calculations are performed for different cases where the damping coefficient  $\gamma$  changes. Fig. 7 shows the graph of mechanical power received by the model as a function of the amplitude of the applied external force.

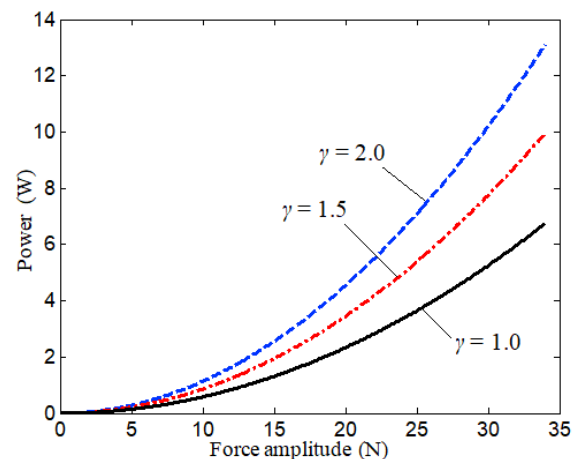


**Figure 7. The graph of mechanical power versus the amplitude of the applied external force**

From the obtained results, it is evident that at small external force amplitudes, the difference in mechanical power received between the cases is small. However, at larger external force amplitudes, the power levels received in different cases exhibit significant differences.

#### 4. TESTING AND DISCUSSION

Based on the numerical simulation results, the device model was fabricated and tested to evaluate the voltage level generated by the mechanical vibrations of the rotating rotor. The parameters of the

model are set up as follows: the beam receives vibration energy from the rotating rotor, with the following specifications - length: 750 mm, width: 20 mm, thickness: 2 mm, mass: 0.3 kg, and material: SKD 11 steel. The permanent magnet shaft on the beam is positioned 450 mm from the machine base. The NdFeB N52 cylindrical magnet has a remanence of 1.4 T, a diameter of 30 mm, and a length of 32 mm. The coil is 25 mm in length with a diameter of 42 mm and consists of 500 turns using copper wire with a diameter of 0.64 mm. It operates with a load of up to 1.54 A, with a maximum temporary increase to 2 A.



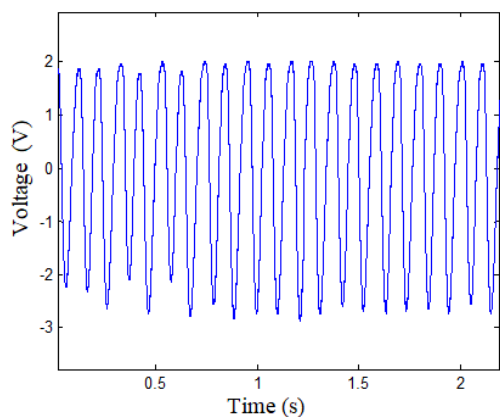
a. Experimental model on rotating rotor



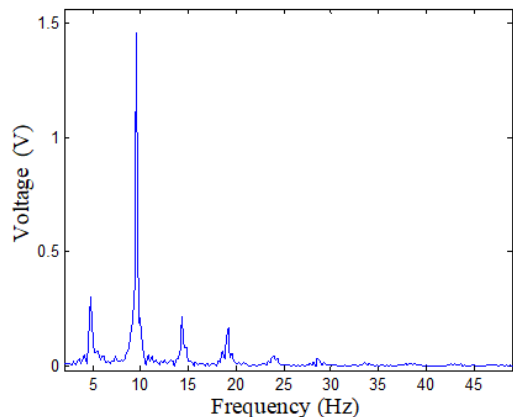
b. LED load output voltage

#### Figure 8. Fabrication and testing of the device prototype

In the experiment, the author used the Picoscope USB oscilloscope 2204A and signal processing software to analyze the output voltage obtained from the device model. In Fig. 9, the output voltage waveform on the load is observed in both the time domain (see Fig. 9a) and the frequency domain (see Fig. 9b).



a. Output load voltage versus time



b. Spectrum of the output load voltage

Figure 9. Output voltage waveform on the load of the device model

From the obtained results, it can be seen that the received voltage level is stable

over time and contains multiple frequency components. Specifically, the voltage level is primarily concentrated at a frequency of 9.7 Hz, with the largest frequency spectrum amplitude reaching 1.47 V and a current of 0.5 A. Additionally, there are also other voltage components at frequencies of 4.9 Hz, 14.6 Hz, and 19.1 Hz, with very small voltage amplitudes.

Based on the experimental results obtained, the author found that the device model can harness the vibration energy of operating devices, particularly high-speed rotating rotors. Additionally, the device model can be installed on high-rise buildings and air traffic towers to generate electricity from mechanical vibrations. The harvested power will serve as an energy source for operating signal lights.

## 5. CONCLUSIONS

In this paper, the author presents the structure of a model for energy harvesting

from mechanical vibrations. This energy harvesting model not only generates electricity for practical use but also mitigates harmful vibrations, contributing to the protection and longevity of machine operating life.

The calculation results have identified the stable and unstable operating regions, the oscillation range, and the power level of the device model, which harnesses mechanical vibrations from the environment.

Based on the obtained calculation results, the author fabricated the device model and tested its operation under the influence of vibrations caused by the rotating rotor. The device generated electricity with a received voltage spectrum amplitude of 1.47 V and a current of 0.5 A. The study results presented in this paper will serve as the scientific basis for calculating, designing, and fabricating energy-harvesting devices for practical applications.

## REFERENCES

- [1] Vijay Laxmi Kalyani, Anjali Piaus, Preksha Vyas. Harvesting Electrical Energy via Vibration Energy and its Applications. *Journal of Management Engineering and Information Technology*, Vol 2, 2015, pp. 9-14.
- [2] Harsh pandey, Ishan khan, Arpan gupta. Walking based wearable mobile phone charger and lightening system. *2014 International Conference on Medical Imaging, m-Health and Emerging Communication Systems (MedCom)*, 2014, pp. 407-411.
- [3] Todd A. Anderson, Daniel W. Sexton. A Vibration Energy Harvesting Sensor Platform for Increased Industrial Efficiency. *Proc. of SPIE Vol. 6174 (2014)*, pp. 1-9.
- [4] Nguyen Nhu Hieu, Nguyen Doan Son, Nguyen Van Hai, Nguyen Dong Anh and Phan Thi Tra My. Nonlinear vibration analysis of a mono-stable energy harvesting system. *Proceeding of the XIV National Scientific Conference on Solid Mechanics*, Ho Chi Minh City (19-20/7/2018), 2019, pp. 252-259.
- [5] Meghashyam Panyam, Mohammed F. Daqaq. Characterizing the effective bandwidth of tri-stable energy harvesters. *Journal of Sound and Vibration*, 386, 2017, pp. 336-358.

- [6] K. H. Nam, Y. D. Chun, Yu-Syn Ha, J. H. Kim. Linear electric generation system to harvest vibration energy from a running vehicle. *Journal of Vibroengineering*, Vol. 19, 2017, pp. 4009-4017.
- [7] Huajie Zou , Fuhai Cai , Jianghua Zhang , Zhenyu Chu. Overview of environmental airflow energy harvesting technology based on piezoelectric effect. *Journal of Vibroengineering*, Vol. 24, 2017, pp. 91-103.
- [8] Ruqi Sun , Waion Wong , Li Cheng. Bi-objective optimal design of an electromagnetic shunt damper for energy harvesting and vibration control. *Mechanical Systems and Signal Processing* 182 (2023) 109571.
- [9] Ashkan Haji Hosseinkloo, Thanh Long Vu, and Konstantin Turitsyn. Optimal control strategies for efficient energy harvesting from ambient vibration. *2015 IEEE 54th Annual Conference on Decision and Control (CDC)*, 2015, pp. 5391-5396.
- [10] Andrew Muscat, Soham Bhattacharya, and Yong Zhu. Electromagnetic Vibrational Energy Harvesters: A Review, *Sensors* 2022, 22, 5555.
- [11] Nguyen Van Khang. Applied Nonlinear Oscillations, *Bachkhoa Publishing House*, Hanoi, 2016.
- [12] Eriksson M., Isberg J., and Leijon M. Hydrodynamic modelling of a direct drive wave energy converter. *International Journal of Engineering Science*, 43, (2005), pp. 1377-1387.
- [13] Nguyen Van Hai, Nguyen Dong Anh, and Nguyen Nhu Hieu. Fabrication and experiment of an electrical generator for sea wave energy. *Vietnam Journal of Science and Technology*, 2017, 55 (6), pp. 780-792.

### Giới thiệu tác giả:



Van Hai Nguyen graduated from Faculty of Physics in VNU University of Science. He got the B.S. and M.S. degree in Physics of electronics in 1998 and 2004, respectively. He received his Ph.D. degree in Engineering Mechanics from Graduate University of Science and Technology (GUST) in 2019. Now he works at Institute of Mechanics, Vietnam Academy of Science and Technology.

His current research interests include nonlinear dynamical systems, numerical simulation, system and control theory, device design and fabrication, and energy harvesting from mechanical vibration.